ARTICLE IN PRESS

Bioorganic & Medicinal Chemistry xxx (xxxx) xxx–xxx

Contents lists available at ScienceDirect

Bioorganic & Medicinal Chemistry

journal homepage: www.elsevier.com/locate/bmc

Anti-acute myeloid leukemia activity of 2-chloro-3-alkyl-1,4-naphthoquinone derivatives through inducing mtDNA damage and GSH depletion

Kun Li[a,1], Kun Yang[a,1], Lifang Zheng[a,*], Yuanyuan Li[a], Qi Wang[b], Ruili Lin[a], Dian He[a,*]

[a] Materia Medica Development Group, School of Pharmacy, Lanzhou University, Lanzhou 730000, China
[b] State Key Laboratory of Applied Organic Chemistry, Lanzhou University, Lanzhou 730000, China

ARTICLE INFO

Keywords:
1,4-Naphthoquinone
Acute myeloid leukemia
Mitochondrial DNA
Mitochondria
GSH

ABSTRACT

2-Chloro-3-alkyl-1,4-naphthoquinone derivatives were synthesized and tested as the anti-acute myeloid leukaemia agents. The compound **9b** (2-chloro-3-ethyl-5,6,7-trimethoxy-1,4-naphthoquinone) was the most potent toward HL-60 leukaemia cells. In mechanistic study for **9b**, the protein levels of mtDNA-specific DNA polymerase γ (poly-γ) and mtDNA transcription factor A (mt-TFA) were decreased after the 24 h treatment, showing the occurrence of mtDNA damage. And **9b** triggered cell cycle arrest at S phase accompanied by a secondary block in G2/M phase which had a direct link to the process of mtDNA damage. The dissipations of mitochondrial membrane potential and ATP also proceeded. On the other hand, **9b** promoted the generation of ROS and resulted in the oxidation of intracellular GSH to GSSG. This process was coupled to the formation of adduct between **9b** and GSH, detected by the UV–Vis spectrum and HRMS analysis. Depletion of GSH by buthionine sulfoximine enhanced ROS level and produced higher cytotoxicity, suggesting GSH was involved in the anti-leukemic mechanism of **9b.** Together, our results provide new insights on the molecular mechanism of the derivatives of 2-chloro-1,4-naphthoquinone and **9b** might be useful for the further development into an anti-leukemia agent.

1. Introduction

Acute myeloid leukaemia (AML) is a malignant hyperplasia and heterogeneous disease characterized by continuous proliferation, inhibition of apoptosis and genetic aberrations, ultimately resulting in the inhibition of normal hematopoiesis.[1–3]

During the development of novel drugs against AML, mitochondria have emerged as a drug target which has manifested the clinical effectiveness in combating relapsed or refractory AML.[3] Cancer mitochondria are structurally and functionally different from their normal counterparts, so cancer cells are more susceptible to mitochondrial perturbations.[4] More importantly, a high frequency of mitochondrial DNA (mtDNA) mutations exists in the AML cells.[5,6] The human mitochondrial genome contains 16.5 kb DNA which encode 13 respiratory chain subunits. As respiratory chain play an important role in mitochondrial ATP generation, drugs that target mtDNA probably will remarkably affect cell viability and cellular physiological function.[7] Besides, mtDNA is more susceptible to the DNA damaging agents, because of the lack of protection by histones and the relatively weak DNA repair capacity in mitochondria.[8] Failure to repair mtDNA damage has demonstrated to initiate cell death by apoptosis.[9]In the case of anti-leukaemia agents, some drugs have a 1,4- naphthoquinone (1,4-NQ) pharmacophore. The representative compounds are shown in Fig. 1. Daunorubicin and doxorubicin have been used clinically for the treatment of AML.[10,11] Plumbagin (5-hydroxy-2-methyl-1,4-naphthoquinone), a naturally occurring naphthoquinone, was much efficient in killing a broad spectrum of leukaemias, with IC_{50} value around 2.0 μM.[12–14] Additionally, the synthetic compounds TW-92 (2-chloro-3-amino-phenyl-1,4-NQ derivative),[15,16] *C*2 (1,4-naphthoquinone-1,2,3-triazole),[17] FNQ3 (2-methyl-naphtho[2,3-*b*]furan-4,9-dione),[18] and BiQ3 (dimeric naphthoquinone)[19] have been documented showing the high cytotoxic activity against leukaemic cells, especially towards AML cells. Recently, we found that the introduction of chlorine atom at C-2 of 1,4-NQ led to the significant enhancement of cytotoxicity.[20]

Obviously, as the anti-AML drugs, 1,4-NQ derivatives have different active functional groups on the quinone scaffold. Hence, cytotoxic

* Corresponding authors.
E-mail addresses: zhenglf@lzu.edu.cn (L. Zheng), Hed@lzu.edu.cn (D. He).
[1] These two authors contributed equally to this article.

https://doi.org/10.1016/j.bmc.2018.07.010
Received 18 May 2018; Received in revised form 4 July 2018; Accepted 6 July 2018

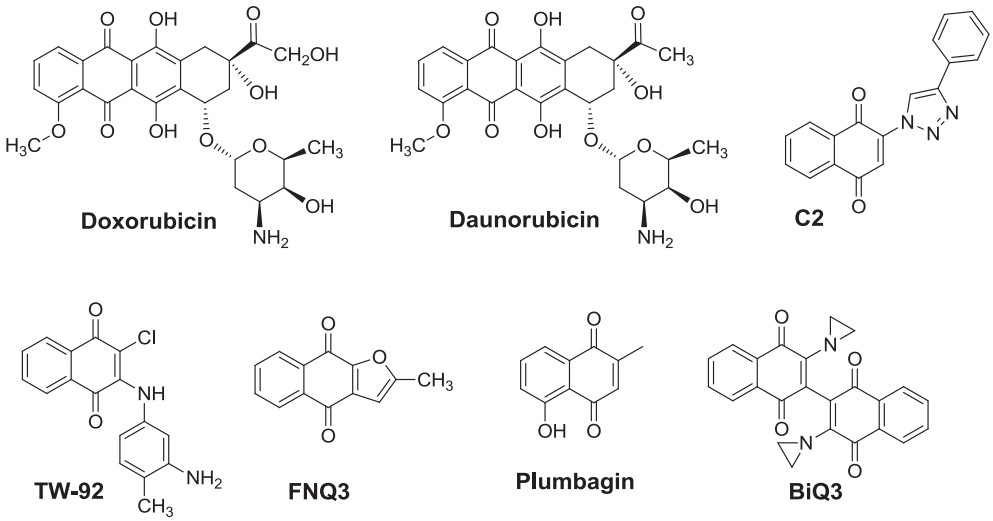

Fig. 1. Quinoid compounds display anti-leukaemia activity.

effects might be mediated by a variety of mechanisms: induce cellular oxidative stress,[12,20] activate mitochondrial apoptotic pathway,[16,18] interact with DNA topoisomerase II,[11] phosphorylate ERK, p38, and JNK kinase,[16,13] regulate thioredoxin reductase[14] and others. On the other hand, cytotoxic effects of 1,4-NQ might be attributed to the alkylation of essential protein thiol or amine groups and/or the oxidation of thiols by reactive oxygen species (ROS).[21] In spite of its undoubted anti-AML activity, the mode of action of 1,4-NQ in mitochondria has been little investigated.

As a continuous study on synthesis and biological evaluation of 1,4-NQ derivatives,[20] we decided to use 2-chloro-1,4-NQ as a core structure and modify the C-3 position with the alkyl side chain while introducing the trimethoxyl substituent on benzene ring. To our knowledge, the methoxyl substituent is an active fragment present in a number of anticancer drugs. Herein, 2-chloro-3-alkyl- 5,6,7-trimethoxy- 1,4-

NQ derivatives were synthesized. All targeted compounds were evaluated for their cytotoxicity against acute myeloid leukemia HL-60 cells and fetal lung fibroblast WI-38 cells using plumbagin and 5-fluorouracil (5-FU) as the positive reference compounds. The anti-AML mechanism was evaluated for the most potent compound **9b**, showing that **9b** induced mtDNA damage, mitochondrial dysfunction, and reduced the intracellular glutathione (GSH) amount.

2. Result

2.1. Chemistry

According to our reported synthetic methods,[20] the title compounds (**9a-9e**) were obtained (Table 1). The compounds (**9a-9e**) were reported herein for the first time and fully characterized by ^{1}H, ^{13}C NMR, and ESI/HRMS. Compound **10** has been reported in our published article.[20] Compound **11** was from J&K Scientific Ltd.

The synthesis of target compounds (**9a-9e**) is illustrated in Scheme 1. Briefly, the 3,4,5-trimethoxybenzaldehyde (**1**) was treated with sodium borohydride to give the 3,4,5-trimethoxybenzyl alcohol (**2**) in excellent yields. Reaction of alcohol **2** with thionyl chloride afforded the 3,4,5-trimethoxybenzyl chloride (**3**), which was further treated with sodium cyanide to yield 3,4,5-trimethoxybenzyl cyanide (**4**). The benzyl cyanide **4** was then hydrolyzed under acidic conditions to give the corresponding phenylacetic acid **5**. Subsequent esterification of **5** gave methyl phenylacetate **6**. The compounds **7a-7e** were obtained through acylating **6** with acyl chloride, in dichloromethane containing $AlCl_3$ as the Lewis acid catalyst. A Claisen condensation reaction was then developed in refluxing sodium methoxide to afford naphthoquinones **8a-8n** after aerial oxidation and acidic workup. The chlorination of **8a-8n** on C-2 hydroxyl group gave **9a-9e.**

2.2. Evaluation of cytotoxicity

We employed 2,5-diphenyltetrazolium bromide (MTT) colorimetric assay to assess the cytotoxicity of the compounds (**9a-9e, 10, 11**) toward acute myeloid leukemia HL-60 cells and the normal cells, fetal lung fibroblast WI-38 cells. The results are listed in Table 1. All the compounds displayed potent cytotoxic activity to HL-60 cells and low toxicity to the normal WI-38 cells. However, they showed less potent or similar cytotoxicity than plumbagin. The selective index (SI) is calculated as the ratio of cytotoxic activity between WI-38 and HL-60 cells after the 48 h treatment. The results revealed that the most active compound **9b** had the higher SI with value of 8.35.

For the compounds (**9a-9e**) bearing tri-methoxyl moiety, they displayed anti-leukemia activity, with the values of IC_{50}/48 h ranging from 2.85 to 12.89 μM. With the elongation of the alkyl side tail at C-3, the activities of **9a-9e** increased in a parabola fashion. Compound **9b** displayed the highest activity, indicating two carbon atoms were the optimum side chain.

Interestingly, it was found that the introduction of methoxyl substituents on benzene ring slightly decreased the cytotoxic activity. After the 48 h treatment, compound **10** containing m-dimethoxyl substituent on benzene ring (IC_{50} = 3.81 ± 0.31 μM) was approximately 1.9 times more active than the corresponding compound **9d** with trimethoxyl substituent (IC_{50} = 7.22 ± 0.74 μM). It was also the case in the comparison of IC_{50} values of compound **9a** (IC_{50} = 10.80 ± 1.66 μM) and compound **11** (IC_{50} = 6.32 ± 0.36 μM), showing compound **11** with none substituent on benzene ring was more active than the corresponding compound **9a** with trimethoxyl substituent. The same observation also has been found after the 24 h treatment.

Finally, the cytotoxicity of **9b** against other cancer cell lines was also tested (Table 2). The cell lines used were: hepatoma (HepG2), cervical carcinoma (HeLa), and lung carcinoma (A549). The results of this screening suggested **9b** might have a broad spectrum of anticancer activity and showed excellent cellular selectivity toward HL-60 cells. Therefore, compound **9b** was selected for the further mechanistic study.

2.3. Arrest cell cycle and damage mtDNA by 9b

The perturbation of cell cycle is closely related to the dysfunction of mitochondria and cytotoxicity.[22,23] To explore whether **9b** might cause the arrest of cell cycle, a flow-cytometric analysis of HL-60 cells stained

Table 1
Cytotoxicity of compounds against HL-60 and WI-38 cells.

Compd.	Structure	IC_{50} (μM)[a]			SI[b]
		HL-60		WI-38	
		24 h 48 h	48 h	48 h	
9a	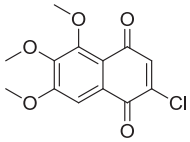	24.74 ± 0.51	10.80 ± 1.54	15.02 ± 1.31	1.39
9b	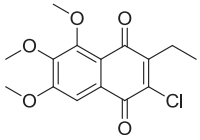	7.65 ± 0.21	2.85 ± 0.29	23.81 ± 0.54	8.07
9c	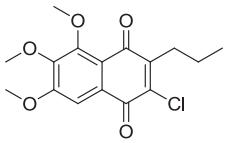	13.61 ± 0.72	3.70 ± 0.15	31.12 ± 0.98	8.38
9d	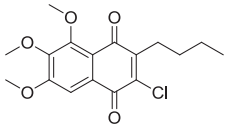	15.43 ± 0.33	7.22 ± 1.12	40.24 ± 2.12	5.54
9e	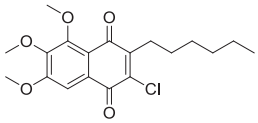	21.04 ± 0.91	12.89 ± 1.46	33.01 ± 1.14	2.56
10	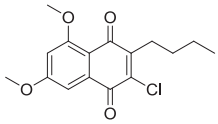	10.19 ± 0.86	3.81 ± 0.31	23.21 ± 0.45	6.04
11	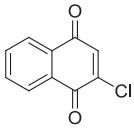	11.48 ± 0.67	6.32 ± 0.21	21.58 ± 0.73	3.32
Plumbagin	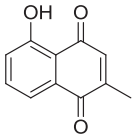	8.25 ± 0.81	3.67 ± 0.53	26.71 ± 0.74	7.28

[a] Values represent mean ± SE from at least three independent experiments.
[b] SI = IC_{50} WI-38 normal cells/IC_{50} HL-60 cancer cells after the 48 h treatment.

with propidium iodide (PI) was performed. After the cells were treated with various concentrations of **9b** (3, 6 and 9 μM) for 24 h, **9b** increased the number of cells in S-phase accompanied by a secondary block in G2/M progression in a dose-dependent manner (Fig. 2A). At 48 post-treatment, the lower concentrations of **9b** (3 μM, 6 μM) enhanced the obvious arrest at G2/M phase along with the moderate arrest at S phase, while the higher concentration of **9b** at 9 μM exclusively caused a significant increase in population of G2/M cells along with loss of cells in G0/G1 and S phases (Fig. 2A). Besides, the percentage of apoptotic cells was also determined using Annexin V-FITC/PI double staining assy. There were the time-dependent and dose-dependent increases in population of early-apoptotic cells (right low section) together with late-apoptotic or necrotic cells (right upper section) (Fig. 2B). We might infer that **9b** mainly induced apoptotic cell death in HL-60 cells.

Specifically, it has reported that the occurrence of S phase arrest along with a moderate G2/M blockade might accompany the damage to mtDNA.[23,24] Hence, we were motivated to investigate whether **9b** could damage mtDNA after the incubation for 24 h in HL-60 cells. The damage to mtDNA may start at transcription and replication levels. The mitochondrial transcription factor A (mt-TFA) is the key activator of mitochondrial transcription as well as a participant in mtDNA replication, mitochondrial biogenesis and cellular metabolism in cells.[25–27] Besides, mitochondrial DNA polymerase gamma protein (poly-γ) is responsible for mtDNA synthesis, replication, and repair of mtDNA damage.[28] We examined poly-γ and mt-TFA expression as the markers of mitochondrial DNA (mtDNA) damage by Western blots (Fig. 2C), expecting that treatment with **9b** would inhibit the protein levels of poly-γ and mt-TFA. Upon the treatment with the various doses (3, 6 and 9 μM) of **9b** for 24 h, there were the significant decreases in mt-TFA and poly-γ levels: the decreases were 71% for mt-TFA level and 32% for poly-γ level at 9 μM over the control groups (Fig. 2D). Together, the inhibition of the protein levels of mt-TFA and poly-γ is consistent with a marked cell cycle arrest in the S phase and a minor arrest in the G2/M phase at 24 h post -treatment, indicating the damage of mtDNA may be

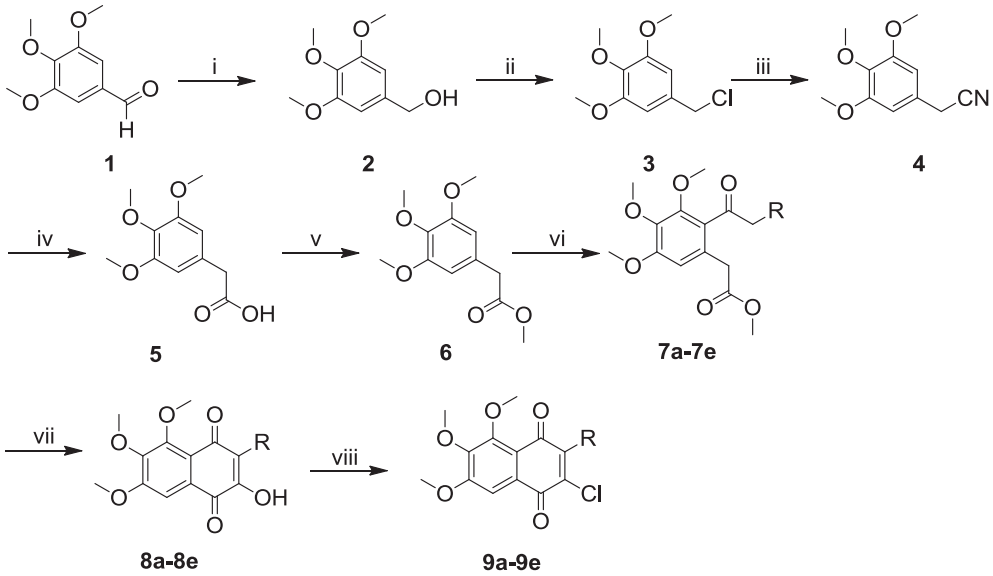

Scheme 1. Reagents and conditions: (i) $NaBH_4$, THF, MeOH, 0 °C, 2 h, 94%; (ii) $SOCl_2$, CH_2Cl_2, rt, 1.5 h, 89%; (iii) NaCN, DMSO, rt, 36 h, 85%; (iv) H_2SO_4, AcOH, H_2O, reflux, 22 h, 82%; (v) MeOH, H_2SO_4, reflux, 3 h, 78%; (vi) RCOCl, $AlCl_3$, Ar_2, 0-rt, 2 h, 70–81%; (vii) MeONa, MeOH, reflux, 40 min; air bubbler, rt, 24 h, 45–58%; (viii) $SOCl_2$, toluene, reflux, 4 h, 40–58%.

Table 2
Cytotoxicity of compound **9b** against three human cancer cell lines.

Compd.	IC_{50} (μM)[a]		
	HepG2	Hela	A549
9b	15.37 ± 0.49	28.17 ± 0.54	17.91 ± 0.74
5-FU	36.62 ± 0.44	30.21 ± 0.27	55.73 ± 0.59

[a] Values represent mean ± SE from at least three independent experiments.

implicated in the cytotoxicity.

Next, we evaluated the cytotoxic activity of **9b** in the mtDNA-deficient HL-60 cells (termed ρ^0 cells). Obviously, HL-60 ρ^0 cells were more resistant than HL-60 cells to the growth suppressive induction after exposure to **9b**, suggesting that mtDNA damage is at least in part involved in the cytotoxic mechanism of action of **9b** (Fig. 2E).

2.4. Induce mitochondrial dysfunction by 9b

Building upon the above results, we sought to determine the impacts of **9b** on mitochondrial functions. The dissipation of mitochondrial membrane potential (MMP) can be detected by the fluorescent probe tetramethylrhodamine methyl ester (TMRE) which accumulates in the mitochondrial matrix in proportion to MMP.[29] As expected, **9b** decreased MMP in a dose and time-dependent manner, as evidenced by the decrease of the mean fluorescence intensity (MFI) (Fig. 3A). The attenuation of MMP was more significant after the 24 h of incubation. In comparison to the control, the treatment of cells with **9b** for 24 h decreased MMP by about 75%, 86% and 87% for 3 μM, 6 μM and 9 μM, respectively.

Next, using the luciferase-luciferin assay for the determination of total amount of cellular ATP, there was an obvious decrease in ATP level in both a dose and time-dependent manner (Fig. 3B). For example, in comparison to the control, the treatment of cells with **9b** for 24 h depleted the level of ATP by about 23%, 38% and 46% for 3 μM, 6 μM and 9 μM, respectively. Therefore, this body of work demonstrates that **9b** caused mitochondrial impairment.

2.5. Induce GSH depletion by 9b

Cellular thiols can either interact with the 1,4-NQ derivatives or neutralize intracellular ROS accumulation, so they have an effect on the cytotoxicity of the 1,4-NQ derivatives.[21] Quantitative quantification of the GSH and glutathione disulfide (GSSG) levels was based on the enzymatic recycling method.[30] Firstly, the effect of **9b** on the amount of intracellular GSH was determined. The results of total glutathione (GSH + GSSG), GSH, and GSSG are shown in Fig. 4A–D. In comparison with the control, the amount of total GSH as well as GSH decreased, while the level of GSSG increased obviously. For example, after exposure to 9 μM of **9b** for 24 h, we observed that (i) GSH was 2.7 nm/mg protein, showing that **9b** decreased the amount of GSH around 6.9 nm/mg protein contrasting to the control; (ii) in particular, the level of GSSG was 0.71 nm/mg protein, showing that only a small fraction (ca. 20%) of GSH lost was converted to GSSG.

This result let us to investigate the possible mechanisms related to GSH depletion. First of all, we tested whether **9b** could trigger cellular ROS over-accumulation and then oxidize GSH to GSSG. The level of ROS was examined by 2′,7′-dichlorofluorescein (DCF) fluorescence assay after the incubation of cells with **9b** for 6 h. **9b** promoted ROS generation in cells remained higher than the control, with evidence of an increase in the green fluorescence intensity (Fig. 4E). In order to test whether a decrease in cellular GSH level could in turn augment ROS level, HL-60 cells were pretreated with buthionine sulfoximine (BSO) to lower the level of GSH.[14] Contrasting to the BSO-untreated cells, exposure to BSO enhanced the level of ROS by **9b**, supporting GSH may act as an antioxidant to scavenge ROS (Fig. 4E). Hence, we might conclude that **9b** could elicit the oxidative stress which might oxidize GSH to GSSG.

Alternatively, the depletion of GSH promoted by **9b** might be partly due to the formation of corresponding conjugate. The interaction between **9b** and GSH was analyzed using the UV–visible absorption spectrum. Addition of GSH induced rapid disappearance of the absorption peak of **9b** centered at 294 nm, accompanied by development of two peaks around 274 and 355 nm and appearance of two isosbestic points at 285 and 317 nm (Fig. 4F). This was further supported by HRMS analysis showing formation of only the 1:1adduct ($[M+H]^+$: 582.1744) between **9b** and GSH (Fig. 4G). We inferred that the formation of adduct involved a direct substitution reaction with lose of HCl, similar to the case of 2,3-dichloro-1,4-naphthoquinone.[31]

Finally, the effect of GSH on the cytotoxicity of **9b** was determined. Depletion of GSH by BSO remarkably augmented the cytotoxicity of **9b** (Fig. 4H), indicating that GSH displayed a protective role against the cytotoxicity of **9b.**

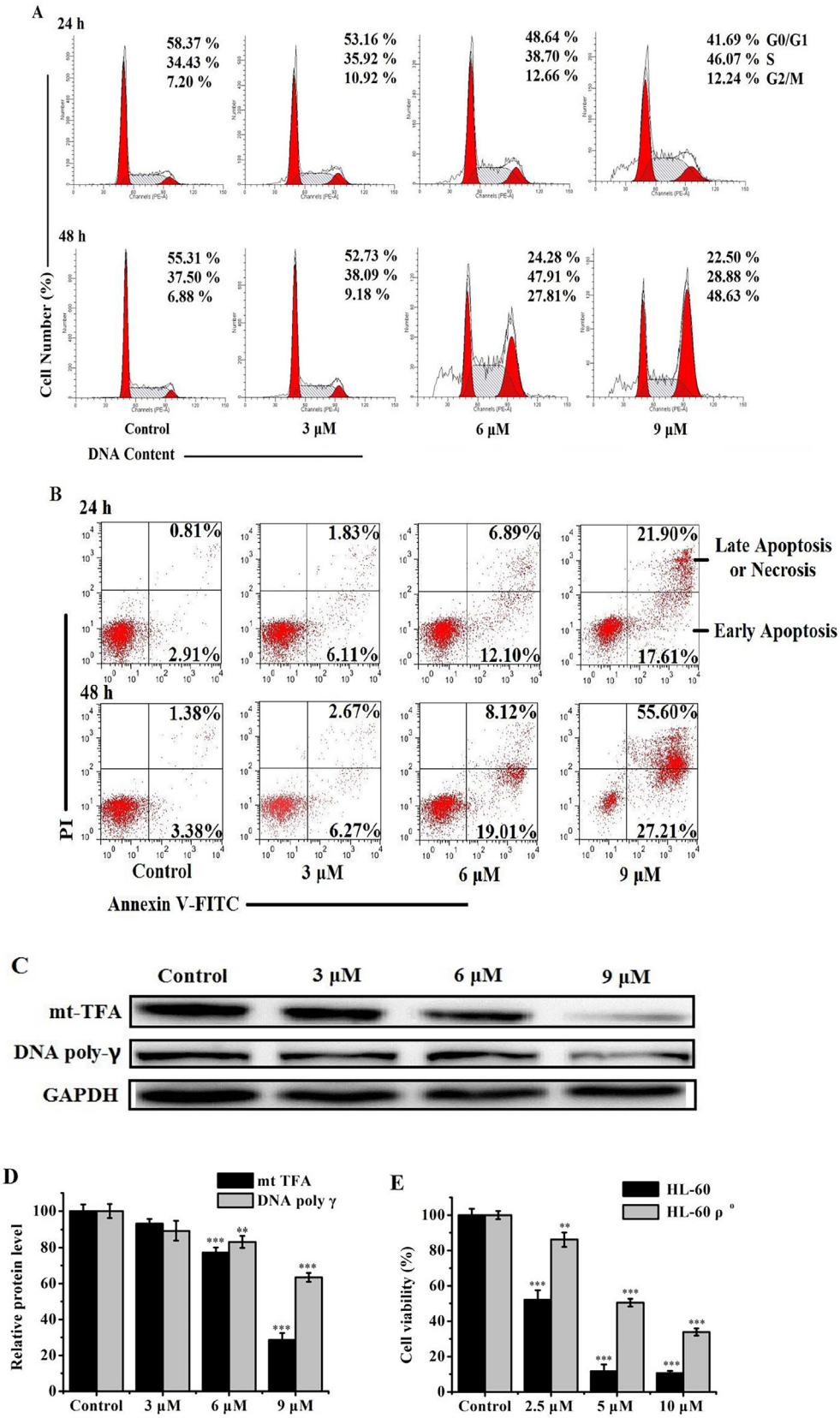

Fig. 2. (A) Analysis of cell cycle arrest by PI staining assay after 24 h and 48 h incubation. (B) Determination of apoptotic percent by Annexin V/PI double-staining assay after 24 h and 48 h incubation. (C) Protein levels of mtDNA transcription factor A (mt-TFA) and mtDNA polymerase gamma (poly-γ) in HL-60 cells after 24 h incubation. The blots shown are representative of three independent experiments demonstrating similar results. (D) The relative protein levels of mt-TFA and poly-γ were determined by IMAGE J software. (E) Concentration-dependent cytotoxicity of **9b** towards HL-60 and HL-60 ρ^0 cells for 48 h. Cell viability was assessed by the MTT method. Data are expressed as mean ± SE from triplicates. $^{***}P < 0.001$, $^{**}P < 0.01$ vs. the control groups.

3. Discussion

In the present study, we reported on the anti-ALM effect and possible mechanism of 2-chloro-5,6, 7-trimethoxy-1,4-NQ analogues containing the alkyl side chain at C-3. Among these compounds, compound **9b** was identified as a promising candidate. The structure-cytotoxic activity relationships (SARs) for the tested compounds were obtained: (i) with the elongation of alkyl tail at C-3, two carbon atoms were the optimum side chain for activity; (ii) introduction of methoxyl substituents on benzene ring slightly decreased the cytotoxicity. Pal et al.

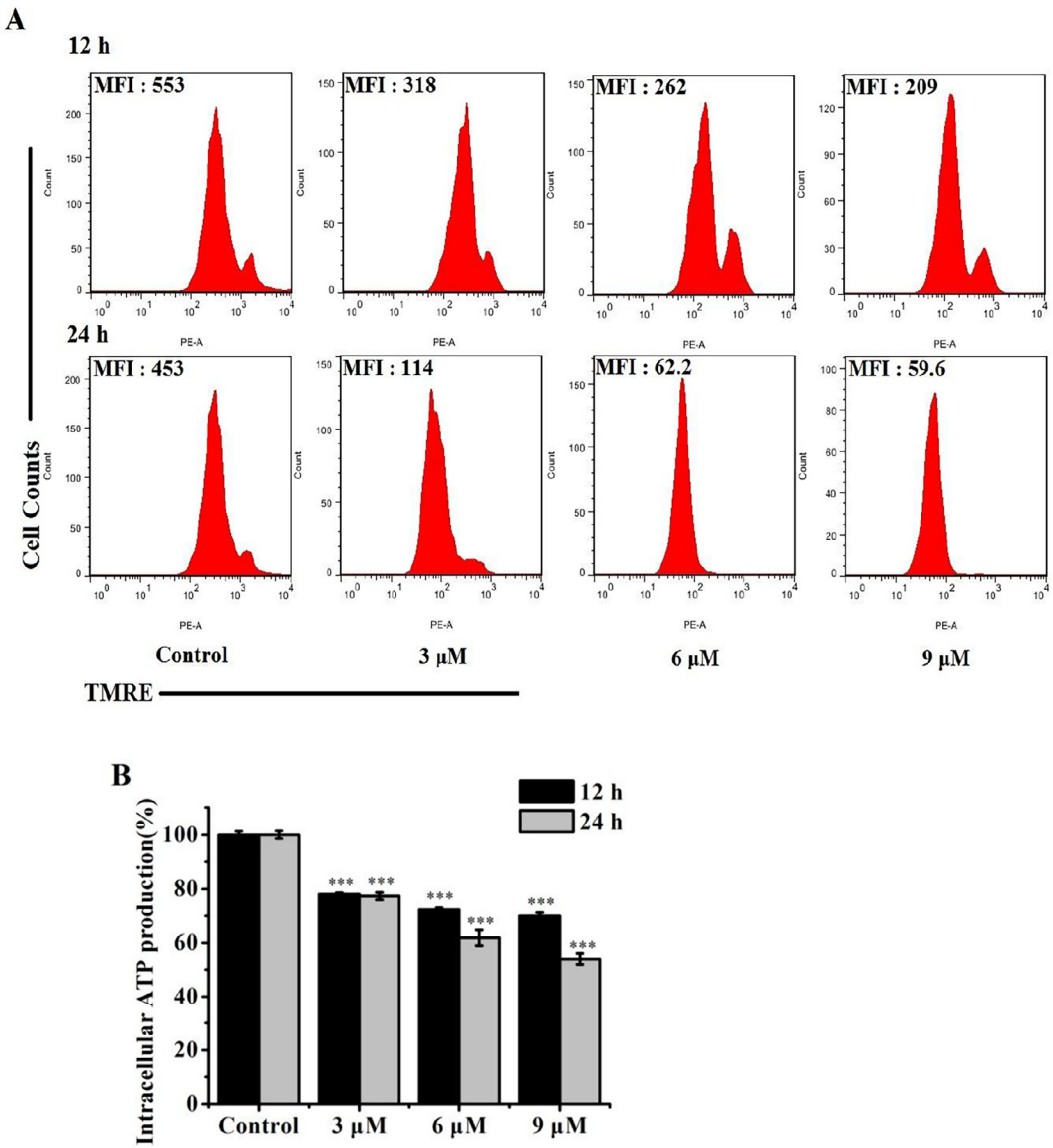

Fig. 3. Induction of mitochondrial dysfunction by **9b** in HL-60 cells after 12 h and 24 h incubation. (A) Determination of MMP by flow cytometry. The data represented as mean fluorescence intensity (MFI) of TMRE probe. (B) Determination of ATP by ATP Assay Kit. Values are expressed as the means ± SE; n = 3, $^{***}P < 0.001$ vs. the control groups.

proposed that the increase in side chain length of the alkyl groups might restrict the interactions of 1,4-NQ derivatives with DNA or other bimolecular, which in turn might decrease cytotoxicity activity.[32] Besides, methoxyl substituent would decrease the redox potential of naphthoquinone/naphthosemiquinone redox couple, which had a negative effect on ROS generation and cytotoxicity activity. We have found that the more positive is the redox potential of the naphthoquinone, the stronger is the cytotoxicity activity.[20] Thus, the cytotoxic effects might be mediated by more than one mechanism.

The promotion of DNA strand scission, alkylation, and the intercalation into DNA, inhibition on DNA topoisomerase I and II are recognized as the prominent mechanisms underlying the anticancer activity of 1, 4-NQ.[33,34] However, few studies have looked into the effect of 1, 4-NQ on mtDNA. Here, we found that **9b** might have an effect on mtDNA. Firstly, after 24 h-post treatment, **9b** increased the number of cells in S-phase accompanied by a secondary block in G2/M progression, indicating the occurrence of damage to mtDNA (Fig. 2A). Koczor et al. reported that damage to mtDNA was shown to activate the cell cycle regulatory kinase, Chk-2, trigger S-phase arrest, and cause a secondary block in G2/M phase.[23] Secondly, as a mark of mtDNA damage, the protein levels of mtDNA-specific DNA poly-γ and mt-TFA were detected by western blots. Exposure of cells to **9b** inhibited the protein levels of poly-γ and mt-TFA, proving the damage of mtDNA (Fig. 2C). Further, involvement of mtDNA damage to the cytotoxicity by **9b** was demonstrated by the mtDNA-deficient HL-60 ρ^0 cells. HL-60 ρ^0 cells were more resistant than HL-60 cells to the growth suppressive induction after exposure to **9b**. Moreover, **9b** also triggered the depolarization of MMP and depletion of ATP in a dose and time-dependent manner, confirming the occurrence of mitochondrial dysfunction (Fig. 3). Taken together, we concluded that **9b** might target mitochondria by damaging mtDNA and causing dysfunction.

The damage to mtDNA may elicit the dysfunction of electron transport chain, which will in turn lead to an increase in mitochondria-generated ROS.[7] ROS are involved in cell death by imposing an oxidative stress. Cellular redox homeostasis can be maintained by the GSH which scavenge excessive production of ROS.[35] GSH also is a major thiol nucleophile in cells, which is important in quinone inactivation by conjugate formation.[21] It was also the case in menadione. In rat platelets, 85% of intracellular GSH was reported to deplete as menadione-GSH conjugate, whereas in hepatocytes, 75% of GSH was depleted by

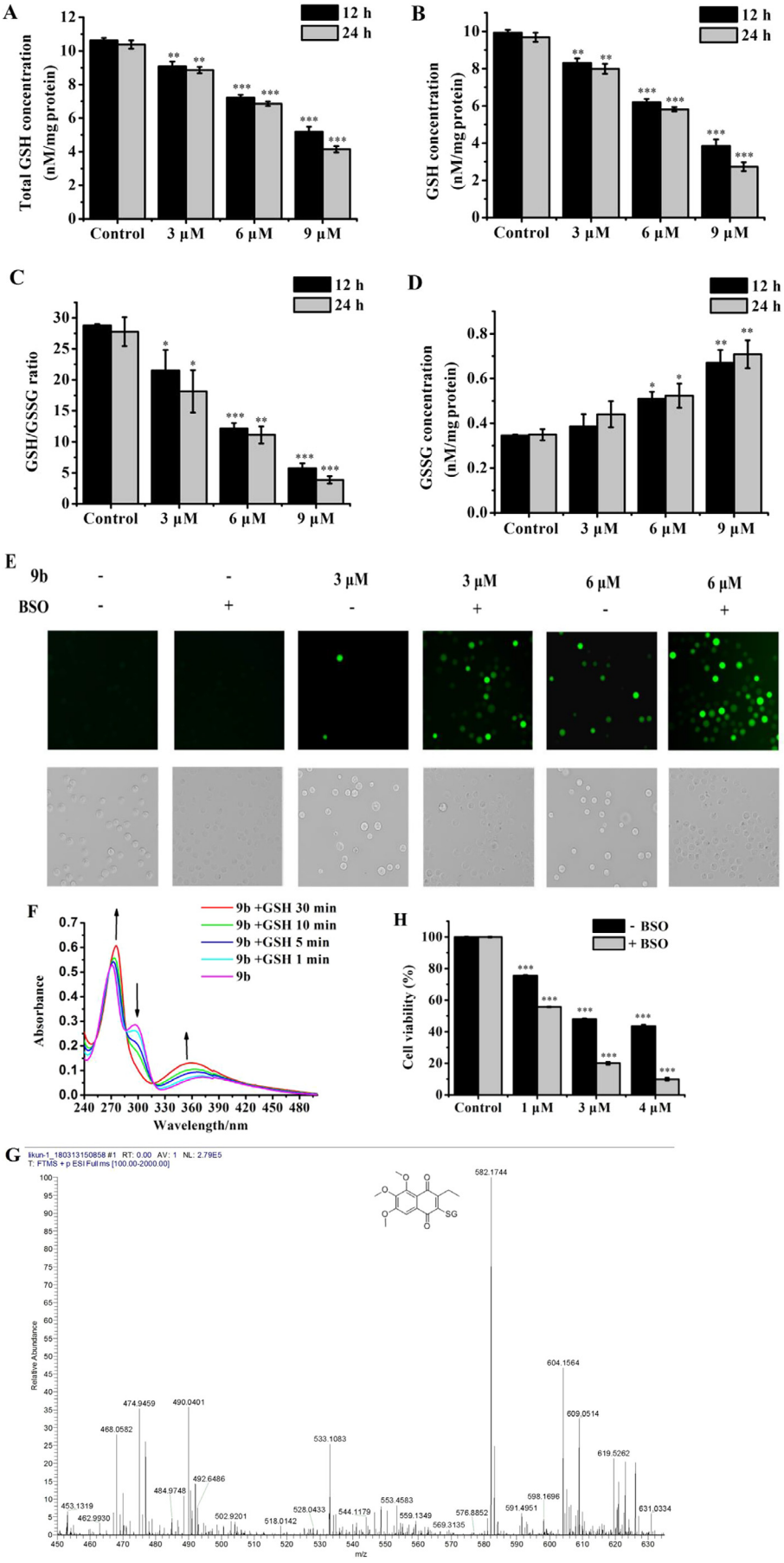

Fig. 4. (A-D) The intracellular concentrations of GSH, total GSH, GSH/GSSG ration and GSSG after 12 h and 24 h incubation. (E) Enhancement of accumulation of ROS in the cells by GSH depletion. HL-60 cells were incubated with 50 μM BSO for 24 h to reduce the intracellular GSH level, followed by **9b** treatment for an additional 6 h. The level of ROS was probed by DCFH-DA. (F) UV–visible absorption spectrum changes for **9b** (50 μM) in the presence of GSH (50 μM) in PBS buffer (pH7.4) at 37 °C. (G) HRMS spectrum of GSH-adduct after mixing **9b** with 1 eq. of GSH at 37 °C for 2 h. (H) Enhancement of the cytotoxicity of **9b** by GSH depletion for 48 h. The cell viability was measured by the MTT assay. Data are expressed as mean ± SE of three experiments. $^{***}P < 0.001$, $^{**}P < 0.01$, $^{*}P < 0.05$ vs. the control groups.

menadione due to formation of GSSG.[36]

We observed that **9b** promoted accumulation of ROS and decreased the level of intracellular GSH and total GSH, including the generation of GSSG (Fig. 4A–E). And 20% of GSH was depleted by **9b** due to formation of GSSG. Importantly, this process was coupled to the formation of adduct between **9b** and GSH, showing by a rapid change of the absorption curve of **9b** (Fig. 4F) and the result of HRMS analysis (Fig. 4G). Thus, we might be sure that the depletion of GSH was due to the formations of GSSG and thioether conjugate. The conjugates might then be degraded to other substances or actively removed from the intracellular media by using an ATP-dependent pump toward thioether conjugate.[37] Additionally, using BSO to lower the level of intracellular GSH augmented the generation of ROS (Fig. 4E) and sensitized the cytotoxicity by **9b** (Fig. 4H), underpinning that GSH may play a detoxifying role.

In summary, we have synthesized 2-chloro-1,4-NQ derivatives (**9a-9e**) and identified compound **9b** as a potent cytotoxic agent against HL-60 cells. Additionally, **9b** also exhibited the moderate cytotoxicity against three selected tumor cell lines (HepG2, Hela, A549) with the IC_{50} values ranging from 15.37 ± 0.49 μM to 28.17 ± 0.54 μM. The SARs have been summarized, suggesting that the structural modification focused on the introduction of electron-withdrawing substituents on the benzene ring may merit exploratory attempt in the future. The mechanistic studied disclosed that the anti-AML action of **9b** was related to its ability to target the mitochondria by inducing mitochondrial dysfunction and damaging mtDNA. Further investigation revealed that **9b** could induce ROS production, GSH depletion and promote GSH-mediated cell death. Clarification of the interaction of **9b** with GSH unveiled the formation of GSH-conjugate, underpinning **9b** might react with tissue nucleophiles to modify proteins covalently. The present results present the possible additional mechanisms underlying the anti-AML effect of naphthoquinone derivative and shed light on considering the development of **9b** as a potential cancer chemotherapeutic agent.

4. Experimental

4.1. Materials and instruments

Reduced glutathione (GSH), 2′,7′-dichlorodihydrofluoresceindiacetate (DCFH-DA), 3-(4,5-dimethylthiazol-2-yl)-2,5-diphenyltetrazolium bromide (MTT) were obtained from Sigma (Beijing, China). Dulbecco's modified Eagle medium (DMEM), fetal bovine serum (FBS) were from Hyclone (Shanghai, China). All antibody were obtained from Santa Cruz Biotechnology (Santa Cruz, CA)). Tetramethylrhodamine ethyl ester (TMRE) were from Biolite Biotech (Tianjin, China). 3,8-diamino-5-ethyl-6-phenylphenanthridinium bromide (EtBr), uridine were obtained from J&K Scientific (Beijing, China). Pyruvate and l-buthionine-(*S*,*R*)-sulfoximine (BSO) were from Solarbio (Beijing, China).

^{1}H NMR and ^{13}C NMR spectra were recorded using a Varian Mercury spectrometer operating at 400 MHz for ^{1}H NMR and 100 MHz for ^{13}C NMR. ESI/HRMS spectra were obtained on an Orbitrap Elite (Thermo Scientific) mass spectrometer Bruker APEX II 47e mass spectrometer.

4.2. Chemistry

The target compounds and intermediates were synthesized according to our previously reported procedures.[20] The products were purified by flash column chromatography, using petroleum ether and ethyl acetate as the eluent. The chemical structures were confirmed by ^{1}H NMR, ^{13}C NMR and ESI/HRMS (supplementary data). The chemical purity of the compounds was determined using a Waters 600 system equipped with a Waters 2998 photodiode array detector, including a 2707 automatic injector and a computer integrating apparatus. The column was a Diamonsil C18 (150 mm x 4.6 mm, 5 μm). The injection volume was 10.0 μL, with detection at 260 nm. The mobile phase was used: methanol: H_2O (80:20, v/v), flow rate of 1 mL/min. The purity of each compound was ≥ 95% in this analysis.

4.2.1. 2-Chloro-5,6,7-trimethoxy-1,4-naphthoquinone (9a)

Yellow solid, M.P. 152.7–153.6 °C, yield 58%; ^{1}H NMR (400 MHz, $CDCl_3$): δ 7.54 (s, 1H), 7.06 (s, 1H), 4.03 (s, 3H), 3.98 (s, 3H), 3.94 (s, 3H); ^{13}C NMR (100 MHz, $CDCl_3$): δ 180.22, 176.87, 156.58, 153.52, 147.72, 142.75, 136.73, 127.55, 118.32, 106.41, 60.87, 60.61, 55.73; HRMS (ESI): found 305.0191 for $[M+Na]^+$ (calcd. For $C_{13}H_{11}ClNaO_5$, 305.0187).

4.2.2. 2-Chloro-3-ethyl-5,6,7-trimethoxy-1,4-naphthoquinone (9b)

Yellow solid, M.P. 88.7–90.2 °C, yield 43%; ^{1}H NMR (400 MHz, $CDCl_3$): δ 7.53 (s, 1H), 4.02 (s, 3H), 3.97 (s, 3H), 3.95 (s, 3H), 2.80 (q, J = 7.5 Hz, 2H), 1.18 (t, J = 7.5 Hz, 3H); ^{13}C NMR (100 MHz, $CDCl_3$)::δ 180.60, 177.68, 157.39, 154.61, 150.98, 148.44, 140.45, 128.61, 119.37, 106.81, 61.65, 61.46, 56.57, 22.27, 12.25; HRMS (ESI): found 311.0682 for $[M + H]^+$ (calcd. For $C_{15}H_{15}ClO_5$, 310.0681).

4.2.3. 2-Chloro-3-propyl-5,6,7-trimethoxy-1,4-naphthoquinone (9c)

Yellow solid, M.P. 64.9–66.2 °C, yield 40%; ^{1}H NMR (400 MHz, $CDCl_3$): δ 7.51 (s, 1H), 3.99 (s, 3H), 3.95 (s, 3H), 3.92 (s, 3H), 2.73 (t, J = 8.0 Hz, 2H), 1.63 – 1.52 (m, 2H), 1.01 (t, J = 7.4 Hz, 3H); ^{13}C NMR (100 MHz, $CDCl_3$): δ 180.66, 177.49, 157.29, 154.52, 149.72, 148.35, 140.68, 128.53, 119.27, 106.71, 61.54, 61.32, 56.47, 30.58, 21.46, 14.35; HRMS (ESI): found 325.0842 for $[M+H]^+$ (calcd. for $C_{16}H_{17}ClO_5$, 3245.0837).

4.2.4. 2-Chloro-3-butyl-5,6,7-trimethoxy-1,4-naphthoquinone (9d)

Yellow solid, M.P. 74.7–76.3 °C, yield 42%; ^{1}H NMR (400 MHz, $CDCl_3$):δ 7.53 (s, 1H), 4.01 (s, 3H), 3.96 (s, 3H), 3.95 (s, 3H), 2.77 (t, J = 7.8 Hz, 2H), 1.57 – 1.42 (m, 4H), 0.95 (t, J = 7.0 Hz, 3H); ^{13}C NMR (100 MHz, $CDCl_3$): δ 180.67, 177.53, 157.30, 154.55, 150.02, 148.36, 140.53, 128.56, 119.30, 106.72, 61.56, 61.34, 56.49, 30.09, 28.54, 23.07, 13.82; HRMS (ESI): found 339.0988 for $[M+H]^+$ (calcd. for $C_{17}H_{19}ClO_5$, 339.0994).

4.2.5. 2-Chloro-3-hexyl-5,6,7-trimethoxy-1,4-naphthoquinone (9e)

Yellow solid, M.P. 46.5–47.6 °C, yield 58%; ^{1}H NMR (400 MHz, $CDCl_3$): δ 7.53 (s, 1H), 4.01 (s, 3H), 3.97 (s, 3H), 3.95 (s, 3H), 2.76 (t, J = 7.8 Hz, 2H), 1.58–1. 50 (m, 2H), 1.46–1. 40 (m, 2H), 1.34–1. 30 (m, 4H), 0.89 (t, J = 7.0 Hz, 3H); ^{13}C NMR (100 MHz, $CDCl_3$):δ 180.91, 177.79, 157.51, 154.75, 150.24, 148.54, 140.74, 128.77, 119.49, 106.93, 61.80, 61.60, 56.73, 31.75, 29.85, 29.04, 28.21, 22.77, 14.31; HRMS (ESI): found 367.1297 for $[M+H]^+$ (calcd. for $C_{19}H_{23}ClO_5$, 367.1307).

4.3. Biological experimental

4.3.1. Cell culture

The cells (HL-60, HepG2, A549, HeLa, and WI-38) were obtained from the Shanghai Institute of Biochemistry and Cell Biology, Chinese Academy of Science. The cells were cultured in DMEM growth medium supplemented with 10% FBS in a humidified 5% CO_2 incubator at 37 °C. The HL-60 ρ^o cells were prepared by treating the cells with 50 ng/ml of EtBr for 14 doublings and documented by lack of mitochondrial EtBr fluorescence.[38]

4.3.2. MTT assay

1×10^4 cells were incubated with the compounds in triplicate in a 96-well plate for the 48 h at 37 °C in a final volume of 100 μL. At the end of the treatment, MTT assay was performed to assess the cell viability. The absorbance was measured at 570 nm using a microplate reader (Thermo Scientific Multiskan GO, Finland).

4.3.3. Apoptosis and cell cycle analysis

5×10^5 HL-60 cells were treated with compound **9b** a in a 6-well

plate for 24 or 48 h.

After that, apoptosis and cell cycle was determined by FITC/PI kit or cell cycle detection kit (Beyotime, Jiangsu, China) using a FACS Canto flow cytometer (Canto, Becton Dickinson, USA).

4.3.4. Western blots

After 5×10^5 HL-60 cells were treated with compound **9** a in a 6-well plate for 24 or 48 h, equal amounts of denatured proteins (20 – 40 μg) were separated by 12% SDS PAGE followed by electroblotting onto polyvinylidene difluoride membranes. Targeted proteins were detected with specific primary antibodies. Corresponding secondary antibodies were then utilized and immunoreactive bands were visualized by fully automatic chemiluminescence analysis system (Tanon, Shanghai, China).

4.3.5. Mitochondrial membrane potential (MMP) detection

After 5×10^5 HL-60 cells were treated with compound **9b** in a 6-well plate for 12 or 24 h, the medium was replaced with fresh medium containing 100 nM of TMRE and incubated for another 30 min at 37 °C. Cells were then washed with PBS buffer (pH 7.4) three times. The fluorescence intensity was quantitatively measured using a FACS Canto flow cytometer at 549 nm excitation and 574 nm emission.

4.3.6. Intracellular ATP detection

Cellular ATP was detected by ATP Assay Kit (Beyotime, Shanghai, China) following the manufacturer's instruction. HL-60 cells were treated with compound **9b** for 12 or 24 h, lysed with ice-cold lysis buffer, and centrifuged at 12000*g* for 10 min at 4 °C. The supernatant was used to assay the ATP level by the detection buffer, and luminescence was measured using a Thermo Varioskan Flash microplate reader.

4.3.7. Intracellular GSH and GSSG detection

The GSH assay is based on the oxidation of GSH by the sulfhydryl reagent 5,5′-dithio-bis(2-nitrobenzoic acid) (DTNB) to form the yellow derivative 5′-thio-2-nitrobenzoic acid (TNB).The rate of formation of TNB, measured at 412 nm, is proportional to the concentration of GSH in the sample. The GSSG formed can be recycled to GSH by glutathione reductase in the presence of NADPH.[30] Briefly, 1×10^6 HL-60 cells were treated with compound **9b** in a 6-well plate for 12 or 24 h. After that, the assay was performed using the GSH and GSSG Assay Kit (Beyotime, Shanghai, China) according to the manufacturer's instructions using a Thermo Varioskan Flash microplate reader.

4.3.8. Intracellular ros assay

After treatment of 5×10^5 HL-60 cells with compound **9b** in a 6-well plate for 6 h, the incubation medium was replaced with the fresh FBS-free medium containing ROS indicator DCFH-DA (10 μM) and incubated for another 30 min at 37 °C in the dark. When necessary, the cells were pretreated with BSO (50 μM) for 24 h to lower the amount of intracellular GSH before adding compound **9b**. The cells were visualized and photographed under an inverted fluorescence microscopy (DMI 4000B, Leica, Germany).

4.3.9. Glutathione conjugate detection

The UV-visible absorption spectrum changes of compound **9b** (50 μM) were recorded in the presence of the equivalent amount of GSH in PBS buffer (pH 7.4) at 37 °C. The formation of conjugate was further determined by ESI/HRMS spectrum. Briefly, **9b** (0.5 mM) was dissolved in methanol (5 mL), and to this solution was added 0.5 mM of GSH dissolved in 5 mL of PBS buffer (pH 7.4). After stirring for 2 h under Ar_2 at 37 °C, the solvent was evaporated and then the molecular mass of conjugate was assayed by HRMS.

4.4. Statistical analysis

The data are expressed as the means ± SE of at least three independent experiments. Statistical differences between two groups were measured by one-way factorial analysis of variance (ANOVA), using Duncan's post hoc test (SPSS 22.0). $P < 0.05$ versus control was used as the criterion for statistical significance.

Acknowledgments

This work was supported by the Fundamental Research Funds for the Central Universities (Grant No. lzujbky-2018-131), the National Natural Science Foundation of China (Grant No. 21302079), and the Lanzhou Science and Technology Bureau Program Funds (Grant No. 2016-3-108, 2018-1-110).

A. Supplementary data

Supplementary data associated with this article can be found, in the online version, at https://doi.org/10.1016/j.bmc.2018.07.010.

References

1. Rowe JM. AML in 2017: advances in clinical practice. *Best Pract Res Clin Hae-matol.* 2017;30:283–286.
2. Wang ZH, Li DD, Chen WL, et al. Targeting protein–protein interaction between MLL1 and reciprocal proteins for leukemia therapy. *Bioorg Med Chem.* 2018;26:356–365.
3. Basak NP, Banerjee S. Mitochondrial dependency in progression of acute myeloid leukemia. *Mitochondrion.* 2015;21:41–48.
4. Weinberg SE, Chandel NS. Targeting mitochondria metabolism for cancer therapy. *Nat Chem Biol.* 2015;11:9–15.
5. Silkjaer T, Norgaard JM, Aggerholm A, et al. Characterization and prognostic significance of mitochondrial DNA variations in acute myeloid leukemia. *Eur J Haematol.* 2013;90:385–396.
6. Sharawat SK, Bakhshi R, Vishnubhatla S, Bakhshi S. Mitochondrial d-loop variations in paediatric acute myeloid leukaemia: a potential prognostic marker. *Br J Haematol.* 2010;149:391–398.
7. Fliss MS, Usadel H, Caballero OL, et al. Facile detection of mitochondrial DNA mutations in tumors and bodily fluids. *Science.* 2000;287:2017–2019.
8. Singh KK, Russell J, Sigala B, et al. Mitochondrial DNA determines the cellular response to cancer therapeutic agents. *Oncogene.* 1999;18:6641–6646.
9. Grishko V, Rachek L, Musiyenko S, et al. Involvement of mtDNA damage in free fatty acid-induced apoptosis. *Free Radic Biol Med.* 2005;38:755–762.
10. Kostrzewa-Nowak D, Paine MJ, Wolf CR, Tarasiuk J. The role of bioreductive activation of doxorubicin in cytotoxic activity against leukaemia HL60-sensitive cell line and its multidrug-resistant sublines. *Br J Cancer.* 2005;93:89–97.
11. Monneret C. Recent developments in the field of antitumor anthracyclines. *Eur J Med Chem.* 2001;36:483–493.
12. Xu KH, Lu DP. Plumbagin induces ROS-mediated apoptosis in human promyelocytic leukemia cells in vivo. *Leuk Res.* 2010;34:658–665.
13. Bae KJ, Lee Y, Kim SA, Kim J. Plumbagin exert an Immunosuppressive effect on human *T*-cell acute lymphoblastic leukemia MOLT-4 cells. *Biochem Biophys Res Commun.* 2016;473:272–277.
14. Zhang J, Peng S, Li X, et al. Targeting thioredoxin reductase by plumbagin contributes to inducing apoptosis of HL-60 cells. *Arch Biochem Biophys.* 2017;619:16–26.
15. Hallak M, Thakur BK, Winn T, et al. Induction of death of leukemia cells by TW-74, a novel derivative of chloro-naphthoquinone. *Anticancer Res.* 2013;3:183–190.
16. Hallak M, Win T, Shpilberg O, et al. The anti-leukaemic activity of novel sy-nthetic naphthoquinones against acute myeloid leukaemia: induction of cell death via the triggering of multiple signaling pathways. *Br J Haematol.* 2009;147:459–470.
17. Coulidiati TH, Dantas BB, Faheina-Martins GV, et al. Distinct effects of novel naphthoquinone-based triazoles in human leukaemic cell lines. *J Pharm Pharmacol.* 2015;67:1682–1695.
18. Desmond JC, Kawabata H, Mueller-Tidow C, et al. The synthetic furanonaphthoquinone induces growth arrest, apoptosis and differentiation in a variety of leukaemias and multiple myeloma cells. *Br J Haematol.* 2005;131:520–529.
19. Carter-Cooper BA, Fletcher S, Ferraris D, et al. Synthesis, characterization and antineoplastic activity of bis-aziridinyl dimeric naphthoquinone – A novel class of compounds with potent Activity against acute myeloid leukemia cells. *Bioorg Med Chem Lett.* 2017;27:6–10.
20. Li K, Wang B, Zheng L, et al. Target ROS to induce apoptosis and cell cycle ar- rest by 5,7-dimethoxy- 1,4-naphthoquinone derivative. *Bioorg Med Chem Lett.* 2018;28:273–277.
21. O'Brien PJ. Molecular mechanisms of quinone toxicity. *Chem Biol Interact.* 1991;80:1–41.
22. Antico Arciuch VG, Elguero ME, Poderoso JJ, Carreras MC. Mitochondrial regulation of cell cycle and proliferation. *Antioxid Redox Signal.* 2012;16:1150–1180.
23. Koczor CA, Shokolenko IN, Boyd AK, et al. Mitochondrial DNA damage initiates a cell cycle arrest by a Chk2-associated mechanism in mammalian cells. *J Biol Chem.* 2009;284:36191–36201.
24. Martinez-Diez M, Santamaria G, Ortega Å.D, Cuezva JM. Biogenesis and dynamics of mitochondria during the cell cycle: significance of 3′UTRs. *PLoS One.* 2006;1:e107.

25. Larsson NG, Wang JM, Wilhelmsson H, et al. Mitochondrial transcription factor A is necessary for mtDNA maintenance and embryogenesis in mice. *Nat Genet.* 1998;18:231–236.
26. Ekstrand MI, Falkenberg M, Rantanen A, et al. Mitochondrial transcription factor A regulates mtDNA copy number in mammals. *Hum Mol Genet.* 2004;13:935–944.
27. Kang D, Kim SH, Hamasaki N. Mitochondrial transcription factor A (TFAM): roles in maintenance of mtDNA and cellular functions. *Mitochondrion.* 2007;7:39–44.
28. Kaguni LS. DNA polymerase gamma, the mitochondrial replicase. *Annu Rev Biochem.* 2004;73:293–320.
29. Scaduto Jr RC, Grotyohann LW. Measurement of mitochondrial membrane potential using fluorescent rhodamine derivatives. *Biophys J.* 1999;76:469–477.
30. Rahman I, Kode A, Biswas SK. Assay for quantitative determination of glutath one and glutathione disulfide levels using enzymatic recycling method. *Nat Protoc.* 2006;1:3159–3165.
31. Nickerson WJ, Falcone G, Strauss G. Studies on quinone-thioethers. I. mechanism of formation and properties of thiodione. *Biochemistry.* 1963;2:537–543.
32. Pal S, Jadhav M, Weyhermüller T, et al. Molecular structures and antiproliferative activity of side-chain saturated and homologated analogs of 2-chloro-3-(*n*-alkylamino)-1,4-napthoquinone. *J Mol Struct.* 2013;1049:355–361.
33. Wellington KW. Understanding cancer and the anticancer activities of naphthoquinones – a review. *RSC Adv.* 2015;5:20309–20338.
34. Kumar BS, Ravi K, Verma AK, et al. Synthesis of pharmacologically important naphthoquinones and anticancer activity of 2-benzyllawsone through DNA topoisomerase-II inhibition. *Bioorg Med Chem.* 2017;25:1364–1373.
35. Schafer FQ, Buettner GR. Redox environment of the cell as viewed through the redox state of the glutathione disulfide/glutathione couple. *Free Radic Biol Med.* 2001;30:1191–1212.
36. Seung SA, Lee JY, Lee MY, et al. The relative importance of oxidative stress versus arylation in the mechanism of quinone-induced cytotoxicity to platelets. *Chem Biol Interact.* 1998;113:133–144.
37. Mauzeroll J, Bard AJ. Scaning electrochemical microscopy of menadione-Glutathione conjugate export from yeast cells. *Proc Natl Acad Sci USA.* 2004;101:7862–7867.
38. Wang XF, Witting PK, Salvatore BA, Neuzil J. Vitamin E analogs trigger apoptosis in HER2/erbB2-overexpressing breast cancer cells by signaling via the mitochondrial pathway. *Biochem Biophys Res Commun.* 2005;326:282–289.